

Filler effects of ZrO₂ nanopowders for improving split tensile damage and pore structure of lightweight cementitious composites

Farzad Soleymani

Department of Metallurgical Engineering, Payame Noor University, P.O. 19395-4697, Tehran, Iran.

E-mail: farzad.soleymani52@yahoo.com

Abstract: Malaysia is the largest producer and exporter of palm oil in the world. However the palm oil refineries also produce tones of waste products known as palm oil clinker or POC. POC is normally disposed of in landfill or incinerated, incurring costs and causing negative environmental impact, such as pollution. Therefore the appropriate use of POC can help preserve the environment from undesirable effects, while at the same time contributes to cost reduction for the palm oil industry. Split tensile of concrete containing ZrO₂ nanoparticles which were cured in saturated limewater have been optimized. ZrO₂ nanoparticles with partial replacement of Portland cement by 0.5, 1.0, 1.5 and 2.0 weight percent have been used as nano-fillers. The specimens were cured in water and saturated limewater for 7, 28 and 90 days after casting and then their strength was evaluated by split tensile strength test. The results showed that replacement of Portland cement with ZrO₂ nanoparticles up to 1.0 weight percent for the specimens cured in water and 2.0% for the specimens cured in saturated limewater produces concrete with the best strength. It has been obtained that curing the specimens in saturated limewater for 28 days and then in water until 90 days, produces more strengthened concrete than those cured only in saturated limewater for 90 days. Excess Ca(OH)₂ crystals which forms after 28 days, when the specimens cured in limewater, reduces the effect of strengthening gels which form until the 90 days hence reduces the mechanical properties of the specimens. On the other hand, curing the specimens in water after 28 days produces more strengthening gel results in a concrete with higher strength. The pore structure of different mixtures was studied. The addition of nanoparticles improves the pore structure of concretes, the refined extent of pore structure increase with decreasing nanoparticles' content. The pore structure of concretes which were cured in saturated limewater is better than that of concretes cured in water.

[Farzad S. Filler effects of ZrO₂ nanopowders for improving split tensile damage and pore structure of lightweight cementitious composites. *J Am Sci* 2012;8(7):240-246]. (ISSN: 1545-1003). <http://www.jofamericansscience.org>. 38

Key words: ZrO₂ nanoparticles; split tensile strength; optimized properties; pore structure; palm oil clinker; lightweight concrete.

POC produced in the boiler when the burning process of husk fiber and shell of palm oil. This burning process is the phase to generate the energy in order to generate the plant boiler in palm oil mill. According to Tay (1991) about 20 % by weight of ash and other residues (i.e. clinker) are produced after the burning process. The clinker turned as abundance of the factory compared to ash. Researches in palm oil industry had been discovered the uses of the palm oil fuel ash (POFA) either as commercial construction material or as fertilizer for the palm oil plant. Also, the ashes turn to potential usage as a detergent. Less of research of POC caused a large amounts of untreated waste and finally contribute of contaminate land, water and air.

There are few reports on incorporation of nanoparticles in cement-based composites. Li et al. [1] investigated the properties of cement mortars blended with nanoparticles to explore their super mechanical and smart (temperature and strain sensing) potentials. Also useful applications of nano-SiO₂ are addressed by the Fuji Chimera Research Institute (2002). However, until now, research

performed over the years has been mainly aimed at achieving high mechanical performance with cement replacement materials in micro level. Several researchers have demonstrated that the finer the SiO₂ particle sizes in micron level, the higher the split tensile strength [2,3]. But there are few works on the effects of ultra fine and nano-size particles on cementitious composite's properties.

Lu and Young [3] achieved high strengths on compressed samples which contain SiO₂ nanoparticles. Richard and Cheyrezy [4] developed Reactive Power Concretes (RPCs) by SiO₂ nano-fillers. The development of an ultrahigh strength cementitious composite was made possible by the application of DSP (Densified System containing homogeneously arranged ultra-fine Particles) with super plasticizer and silica fume content [5]. Kuo et al. [6] investigated the properties of waterworks sludge ash cement paste incorporating SiO₂ nanoparticles. In their work, the flowability of the cement pastes has been considered and it has been shown that the flowability of the cementitious composite decreases by increasing the nanoparticle

amount. Lin and Tsai [7] investigated the influences of nano-materials on the microstructures of sludge ash cement paste. They noticed that the amount of crystallization in the hydrates increased with the increased quantities of nano-material added. Furthermore, denser crystallizations, smaller pore sizes, and a decreased number of pores were observed with the addition of nano-material results in decreasing water permeability.

Table 1. Chemical and physical properties of Portland cement (*Wt. %*)

Material	SiO ₂	Al ₂ O ₃	Fe ₂ O ₃	CaO	MgO	SO ₃	Na ₂ O	K ₂ O	Loss on ignition
Cement	21.8	5.3	3.34	53.2	6.45	3.67	0.18	0.9	3.21

Specific gravity: 1.7 g/cm³

Table 2. The properties of nano-ZrO₂

Diameter (nm)	Surface Volume ratio (m ² /g)	Density (g/cm ³)	Purity (%)
15 ± 3	160 ± 12	< 0.14	>99.9

Table 3. Mixture proportion of nano-ZrO₂ particles blended concretes

Sample designation	nano-ZrO ₂ particles	Quantities (kg/m ³)	
		Cement	ZrO ₂ nanoparticles
C0 (control)	0	450	0
N1	0.5	447.75	2.25
N2	1.0	445.50	4.50
N3	1.5	443.25	6.75
N4	2.0	441.00	9.00

Water to binder [cement + nano-ZrO₂] ratio of 0.40, sand 492 kg/m³, and aggregate 1148 kg/m³

There are few works about incorporating other nanoparticles in cementitious composites. For example, Li et al. [9, 10] have investigated the split tensile strength and aberration resistance of cement paste composites incorporating nano-Fe₂O₃ and nano-TiO₂ particles, respectively. Incorporation of zinc-iron oxide nanoparticles as a replacement of cement have been investigated by Flores-Velez and Dominguez [11].

The other nanoparticles (such as ZrO₂ nanoparticles in this work) have rarely investigated and some of researchers do not agree that the other nanoparticles could be pozzolans. It seems that several works are needed to introduce these new materials as cement replacement.

Previously, a series of works [12-19] has been

conducted on cementitious composites containing different nanoparticles evaluating the mechanical properties of the composites. In this work, the influence of nano-ZrO₂ on split tensile strength of binary blended cementitious composite cured in water and saturated limewater for different ages has been investigated. The optimum replacement level of ZrO₂ nanoparticles has been determined in different curing media has been obtained and the method for achieving the optimum strength using a combination of two curing media has been discussed.

2. Materials and Methods

Ordinary Portland Cement (OPC) obtained from Holcim Cement Manufacturing Company of Malaysia conforming to ASTM C150 [20] standard was used as received. The chemical and physical properties of the cement are shown in Table 1. Also, the distribution pattern of cement obtained from BET method has been illustrated in Fig. 1.

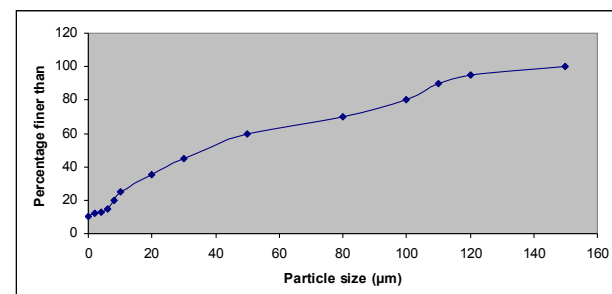


Fig. 1. Illustration of cement particles' distribution.

Nano-ZrO₂ with average particle size of 15 nm prepared from Suzhou Fuer Import & Export Trade Co., Ltd was used as received. The properties of nano-ZrO₂ particles are shown in Table 2.

The clinkers forms are usually flaky and irregular with rough and spiky broken edges. The POC for this study was collected from a palm oil mill factory located at Kahang, Kluang. To ensure a better bonding with the clay, the clinker has been ground to powder form before combined together with clay and cement.

Two series of mixtures were prepared in the laboratory trials. Series C0 mixtures were prepared as control specimens. The control mixtures were made of natural aggregates, cement and water. Series N were prepared with different contents of nano-ZrO₂ particles with average particle size of 15 nm. The mixtures were prepared with the cement replacement of 0.5%, 1.0%, 1.5% and 2.0% by weight. The water to binder ratio for all mixtures was set at 0.40 [21]. The aggregates for the mixtures consisted of a combination of crushed basalt and of fine sand, with the sand percentage of 30% by weight. The binder content of all mixtures was 450 kg/m³. The

proportions of the mixtures are presented in Table 3.

Series N mixtures were prepared by mixing the coarse aggregates, fine aggregates and powder materials (cement and nano-ZrO₂ particles) in a laboratory concrete drum mixer. The powder material in the series C0 mixtures was only cement. They were mixed in dry condition for two minutes, and for another three minutes after adding the water. Cylindrical specimens with the diameter of 150 mm and the height of 300 mm for split tensile strength tests were cast and compacted in two layers on a vibrating table, where each layer was vibrated for 10 s [22]. The moulds were covered with polyethylene sheets and moistened for 24 h. Then the specimens were demoulded and cured in water (N-W series) and saturated limewater (N-LW series) at a temperature of 20° C prior to test days. The strength tests of the concrete samples were determined at 7, 28 and 90 days. A series of the specimens were cured in saturated limewater for 28 days and then cured in water until 90 days (N-LW-W series) after casting and then were tested.

Split tensile test were done in accordance to the ASTM C496 [23] Standard. Again, split tensile tests were carried out on triplicate specimens and average split tensile strength values were obtained.

There are several methods generally used to measure the pore structure, such as optics method, mercury intrusion porosimetry (MIP), helium flow and gas adsorption [24]. MIP technique is extensively used to characterize the pore structure in porous material as a result of its simplicity, quickness and wide measuring range of pore diameter [24, 25]. MIP provides information about the connectivity of pores [24]. In this study, the pore structure of concrete is evaluated by using MIP.

To prepare the samples for MIP measurement, the concrete specimens after 28 days of curing are first broken into smaller pieces, and then the cement paste fragments selected from the center of prisms are used to measure pore structure. The samples are immersed in acetone to stop hydration as fast as possible. Before mercury intrusion test, the samples are dried in an oven at about 110°C until constant weight to remove moisture in the pores.

MIP is based on the assumption that the non-wetting liquid mercury (the contact angle between mercury and solid is greater than 90°) will only intrude in the pores of porous material under pressure [24, 25]. Each pore size is quantitatively determined from the relationship between the volume of intruded mercury and the applied pressure [25]. The relationship between the pore diameter and applied pressure is generally described by Washburn equation as follows [24, 25]:

$$D = -4\gamma \cos\theta / P \quad (1)$$

where, D is the pore diameter (nm), γ is the surface tension of mercury (dyne/cm), θ is the contact angle between mercury and solid (°) and P is the applied pressure (MPa).

The test apparatus used for pore structure measurement is AutoPore III mercury porosimeter. Mercury density is 13.5335 g/ml. The surface tension of mercury is taken as 485 dynes/cm, and the contact angle selected is 130°. The maximum measuring pressure applied is 200 MPa (30000 psi), which means that the smallest pore diameter that can be measured reaches about 6 nm (on the assumption that all pores have cylindrical shape).

3. Results and discussion

3.1. Split tensile strength

The split tensile strength results of series C0-W and N-W mixtures are shown in Table 4. Comparison of the results from the 7, 28 and 90 days samples shows that the split tensile strength increases with nano-ZrO₂ particles up to 1.0% replacement (N2-W) and then it decreases, although the results of 2.0% replacement (N4-W) is still higher than those of the plain cement concrete (C0-W). It was shown that the use of 2.0% nano-ZrO₂ particles in N-W series decreases the split tensile strength to a value which is near to the control concrete. This may be due to the fact that the quantity of nano-ZrO₂ particles (pozzolan) present in the mix is higher than the amount required to combine with the liberated lime during the process of hydration thus leading to excess silica leaching out and causing a deficiency in strength as it replaces part of the cementitious material but does not contribute to strength [26]. Also, it may be due to the defects generated in dispersion of nanoparticles that causes weak zones. The high enhancement of split tensile strength in the N series blended concrete are due to the rapid consuming of Ca(OH)₂ which was formed during hydration of Portland cement specially at early ages related to the high reactivity of nano-ZrO₂ particles. As a consequence, the hydration of cement is accelerated and larger volumes of reaction products are formed. Also nano-ZrO₂ particles recover the particle packing density of the blended cement, directing to a reduced volume of larger pores in the cement paste.

Table 4 also shows the split tensile strength of C0-LW and N-LW series. The results show that the replacement of cement by ZrO₂ nanoparticles up to 2.0 Wt% (N4-LW) in N-LW series produces concrete with high strength with respect to N-LW concrete. By comparison the split tensile strength results of C0-W and C0-LW series, it shows that after 7, 28 and 90 days of curing the concrete in the saturated limewater, the split tensile strength of the C0-LW

series is smaller than the corresponding strength of C0-W series. This may be due to more formation of crystalline $\text{Ca}(\text{OH})_2$ in the presence of limewater which reduces the split tensile strength in C0-LW series with respect to C0-W series. On the other hand, the split tensile strength of the N-LW series is more than those of N-W series. Lime reacts with water and produces $\text{Ca}(\text{OH})_2$ which needs to form strengthening gel. When ZrO_2 nanoparticles react with $\text{Ca}(\text{OH})_2$ produced from saturated limewater, the content of strengthening gel is increased because of high free energy of nanoparticles which reduces significantly when reacts by $\text{Ca}(\text{OH})_2$. The split tensile strength of N-W and N-LW series should be compared from two viewpoints. The first viewpoint is that the split tensile strength of N-

LW series increases by partial replacement of cement with ZrO_2 nanoparticles up to 2.0 wt% (N4-LW) while for N-W series it increases by partial replacement of cement with ZrO_2 nanoparticles up to

1.0 wt% (N2-W) and then decreases. Once more this confirm the more strengthening gel formation in the presence of saturated limewater in which the quantity of nano- ZrO_2 particles (pozzolan) present in the mix is close to the amount required to combine with the liberated lime during the process of hydration thus leading to lesser silica leaching out with respect to the specimens cured in water. Second viewpoint is that the difference between split tensile strengths of the N-W and N-LW series after 28 days of curing is relatively high while this difference in split tensile strength after 90 days of curing is not high. This may be due to formation of crystalline $\text{Ca}(\text{OH})_2$ in N-LW series after the 28 day causes reduction in split tensile strength. In the other words, curing of the ZrO_2 nanoparticles blended concrete in saturated limewater after 28 days is completely suitable to achieve high strength especially with high weight percent of nanoparticles.

Table 4. Split tensile strength of nano- ZrO_2 particle blended cement mortars

Sample designation	nano- ZrO_2 particle (%)	Split tensile strength (MPa)		
		7 days	28 days	90 days
C0-W (control)	0	1.5	1.8	2.3
N1-W	0.5	2.3	2.7	3.2
N2-W	1.0	2.8	3.1	3.4
N3-W	1.5	2.7	2.8	3.0
N4-W	2.0	1.9	1.9	2.2
C0-LW (control)	0	1.3	1.5	1.9
N1-LW	0.5	2.5	3.1	3.1
N2-LW	1.0	3.3	3.4	3.5
N3-LW	1.5	3.7	3.6	3.6
N4-LW	2.0	4.0	3.8	3.8
C0-LW-W (control)	0	1.3	1.5	1.6
N1-LW-W	0.5	2.5	3.1	3.5
N2-LW-W	1.0	3.3	3.4	3.8
N3-LW-W	1.5	3.7	3.6	4.2
N4-LW-W	2.0	4.0	3.8	4.5

Water to binder [cement + nano- ZrO_2] ratio of 0.40

W denotes the specimens cured in water and LW denotes to those cured in saturated limewater

Table 5. Total specific pore volumes and most probable pore diameters of concretes.

Mixture type	Total specific pore volume		Most probable pore diameter	
	Value (mL/g)	Reduced extent (%)	Value (mL/g)	Reduced extent (%)
C0-W (control)	0.0481	0	42	0
N1-W	0.0446	+7.12	34	+19.05
N2-W	0.0451	+6.18	35	+16.67
N3-W	0.0455	+5.24	36	+14.29
N4-W	0.0460	+4.31	39	+7.14
C0-LW (control)	0.0466	0	40	0
N1-LW	0.0426	+8.69	30	+25
N2-LW	0.0431	+7.53	31	+22.5
N3-LW	0.0437	+6.18	34	+15
N4-LW	0.0442	+5.21	36	+10

Water to binder [cement + nano- ZrO_2] ratio of 0.40

W denotes the specimens cured in water and LW denotes to those cured in saturated limewater

Table 6. Prosities, average diameters and median diameters (volume) of concretes.

Mixture type	Prosity		Average diameter		Median diameter (volume)	
	Value (%)	Reduced extent (%)	Value (nm)	Reduced extent (%)	Value (nm)	Reduced extent (%)
C0-W (control)	9.99	0	37.53	0	51.4	0
N1-W	9.01	+8.84	31.9	+13.60	42.5	+15.60
N2-W	9.30	+6.24	34.0	+8.42	44.8	+11.51
N3-W	9.46	+4.78	35.6	+4.75	47.9	+6.15
N4-W	9.56	+3.89	37.1	+1.08	50.4	+1.73
C0-LW (control)	9.66	0	34.2	0	48.7	0
N1-LW	8.20	+13.59	30.1	+10.89	40.1	+15.97
N2-LW	8.42	+11.49	32.3	+4.97	42.4	+11.65
N3-LW	8.70	+8.89	33.0	+3.08	44.3	+8.15
N4-LW	8.90	+7.046	35.4	-3.08	47.9	+1.50

Water to binder [cement + nano-ZrO₂] ratio of 0.40

W denotes the specimens cured in water and LW denotes to those cured in saturated limewater

Table 7. Pore size distribution of concretes

Mixture type	Pore size distribution (mL/g(%))				Total specific pore volume (mL/g)
	Harmless pores (<20 nm)	Few-harm pores (20~50 nm)	Harmful pores (50~200 nm)	Multi-harm pores (>200 nm)	
C0-W (control)	0.0065	0.0147	0.0169	0.0099	0.0481
N1-W	0.0066	0.0166	0.0141	0.0076	0.0446
N2-W	0.0067	0.0161	0.0148	0.0080	0.0451
N3-W	0.0068	0.0156	0.0154	0.0085	0.0455
N4-W	0.0068	0.0151	0.0158	0.0089	0.0460
C0-LW (control)	0.0067	0.0157	0.0148	0.0091	0.0466
N1-LW	0.0069	0.0175	0.0122	0.0064	0.0426
N2-LW	0.0069	0.0170	0.0128	0.0068	0.0431
N3-LW	0.0069	0.0166	0.0140	0.0071	0.0437
N4-LW	0.0070	0.0160	0.0142	0.0075	0.0442

Water to binder [cement + nano-ZrO₂] ratio of 0.40

W denotes the specimens cured in water and LW denotes to those cured in saturated limewater

3.2. Pore structure of concrete

The pore structure of concrete is the general embodiment of porosity, pore size distribution, pore scale and pore geometry. The test results of MIP in this study include the pore structure parameters such as total specific pore volume, most probable pore diameter, pore size distribution, porosity, average diameter, and median diameter (volume).

In terms of the different effect of pore size on concrete performance, the pore in concrete is classified as harmless pore (<20 nm), few-harm pore (20~50 nm), harmful pore (50~200 nm) and multi-harm pore (>200 nm) [27]. In order to analyze and compare conveniently, the pore structure of concrete is divided into four ranges according to this sort method in this work.

3.2.1 Total specific pore volume and most

probable pore diameter of concrete

Table 5 shows that with the addition of nanoparticles, the total specific pore volumes of concretes is decreased, and the most probable pore diameters of concretes shift to smaller pores and fall in the range of few-harm pore, which indicates that the addition of nanoparticles refines the pore structure of concretes.

The effectiveness of nano-ZrO₂ in reducing the total specific pore volumes and most probable pore diameters of concretes increases in the order: N4-LW<N3-LW<N2-LW<N1-LW, and the similar results can be observed for the concretes containing nano-ZrO₂ which were cured in water; i.e. N4-W<N3-W<N2-W<N1-W.

With increasing content of nanoparticles, the reduced extent of total specific pore volume and most probable pore diameter decreases, and the refinement

on the pore structure of concretes is weakening.

Table 6 gives the porosities, average diameters and median diameters (volume) of various concretes. The regularity of porosity is similar to that of total specific pore volume. The regularity of average diameter and median diameter (volume) is similar to that of most probable pore diameter. Therefore, it is no longer necessary to analyze one by one herein.

3.2.2 Pore size distribution of concrete

The pore size distribution of concretes is shown in Table 7. Fig. 2 shows the percent of specific pore volume of various grade pore size accounting for total specific pore volume. It can be seen that by the addition of nano-particles, the amounts of harmless and few-harm pores in concretes increase, and the amounts of harmful and multi-harm pores decrease, which shows that the density of concretes is increased and the pore structure is improved.

The effectiveness of nano-ZrO₂ in improving the pore structure of concretes increases in the order: N4-LW<N3-LW<N2-LW<N1-LW, and the similar results can be observed for the concretes containing nano-ZrO₂ which were cured in water; i.e. N4-W<N3-W<N2-W<N1-W. The harmless and few-harm pores in N1-Lw and N1-W series increase by the largest extent, while its harmful and multi-harm pores decrease by the largest extent, which indicates that the pore structure of N1-Lw and N1-W is most significantly improved. With increasing of nanoparticles' content, the enhanced extent of harmless and few-harm pores and the reduced extent of harmful and multi-harm pores in concretes are all decreased, and the improvement on the pore structure of concretes is weakening.

The mechanism that the nanoparticles improve the pore structure of concrete can be interpreted as follows. Supposed that nanoparticles are uniformly dispersed in concrete and each particle is contained in a cube pattern, the distance between nanoparticles can be determined. After hydration begins, hydrate products diffuse and envelop nanoparticles as kernel. If the content of nanoparticles and the distance between them are appropriate, the crystallization will be controlled to be a suitable state through restricting the growth of Ca(OH)₂ crystal by nanoparticles. Moreover, the nanoparticles located in cement paste as kernel can further promote cement hydration due to their high activity. This makes the cement matrix more homogeneous and compact. Consequently, the pore structure of concrete is improved evidently such as the concrete containing nano-ZrO₂ in the amount of 1% by weight of binder.

With increasing content of nanoparticles, the improvement on the pore structure of concrete is weakening. This can be attributed to that the distance

between nanoparticles decreases with increasing content of nanoparticles, and Ca(OH)₂ crystal cannot grow up enough due to limited space and the crystal quantity is decreased, which leads to the ratio of crystal to strengthening gel small and the shrinkage and creep of cement matrix increased [28], thus the pore structure of cement matrix is looser relatively.

On the whole, the addition of nanoparticles improves the pore structure of concrete. On the one hand, nanoparticles can act as a filler to enhance the density of concrete, which leads to the porosity of concrete reduced significantly. On the other hand, nanoparticles can not only act as an activator to accelerate cement hydration due to their high activity, but also act as a kernel in cement paste which makes the size of Ca(OH)₂ crystal smaller and the tropism more stochastic.

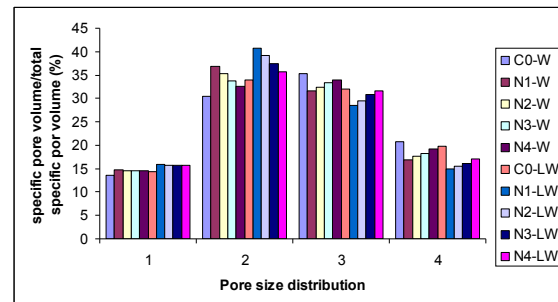


Fig. 2. Percent of specific pore volume of various grade pore size accounting for total specific pore volume.

3.4. Optimized Strength

Table 4 shows the split tensile strength of N-LW-W series blended concretes. The strength of the N-LW-W series is more than that of N-LW series after 90 days of curing. As it mentioned above, this may be due to formation of crystalline Ca(OH)₂ in N-LW series after the 28 day. After curing for 28 days in saturated limewater, curing the specimens in water prevents from crystalline Ca(OH)₂ formation hence produces concrete with higher strength. In the other words, after 28 days of curing in saturated limewater, only strengthening gel forms by curing the specimens until the day 90 in water.

Therefore, the optimized strength of nanoparticles blended concrete was achieved by partial replacement of 2.0 wt% cement with ZrO₂ nanoparticles which was cured for 28 days in saturated limewater and then in water until 90 days.

Conclusions

The results show that the nano-ZrO₂ particles blended concrete had significantly higher strength with respect to that of the concrete without nano-ZrO₂ particles. It is found that the Portland cement could be advantageously replaced with nano-ZrO₂.

particles up to maximum limit of 2.0% with average particle sizes of 15 nm when the specimens cured at saturated limewater for 28 days. The optimal level of nano-ZrO₂ particles content was achieved with 1.0% replacement for the specimens cured in water 7, 28 and 90 days. The optimized strength of nanoparticles blended concrete was achieved by partial replacement of 2.0 wt% cement with ZrO₂ nanoparticles which was cured for 28 days in saturated limewater and then in water until 90 days.

References

- [1] Li H, Xiao HG, Yuan J, Ou J. Microstructure of cement mortar with nano-particles. Composites Part B: Engineering 2003; 35(March).
- [2] Erdogdu K, Tucker P. Effects of fly ash particle size on strength of Portland cement fly ash mortars. Cem Concr Res 1998;28:1217-22.
- [3] Lee SH, Sakai E, Diamond M, Bang WK. Characterization of fly ash directly from electrostatic precipitator. Cem Concr Res 1999;29:1791-7.
- [4] Lu P, Young JF. Hot pressed DSP cement paste, Material Research Society Symposium Proceedings, 1992; 245.
- [5] Richard P, Cheyrezy M. Reactive powder concretes with high ductility and 200- 800 MPa split tensile strength, San Francisco: ACI Spring Convention, SP 144-24, 1994.
- [6] Jo BW, Kim CH, Tae G, Park JB. Characteristics of cement mortar with nano-SiO₂ particles. Const Build Mater 2007; 21(6): 1351-1355.
- [7] Kuo WT, Lin KL, Chang WC, Luo HL, Effects of Nano-Materials on Properties of Waterworks Sludge Ash Cement Paste. Journal of Indian Engineering Chemistry 200; 12(5): 702-709.
- [8] Lin DF, Tsai MC. *Journal of Air Waste Management Assoc*;2006; **56**: 1146.
- [9] Li H, Xiao H. and Ou J. A study on mechanical and pressure-sensitive properties of cement mortar with nanoparticle materials, Cement and Concrete Research 34 (2004) 435-438.
- [10] Li H., Zhang M. and Ou J. Abrasion resistance of concrete containing nano-particles for pavement, Wear 260 (2006) 1262-1266.
- [11] Flores-Velez and Dominguez. Characterization and properties of Portland cement composites incorporating zinc-iron oxide nanoparticles, J Mater Sci 37 (2002) 983- 988.
- [12] Nazari A, Riahi Sh, Riahi Sh, Shamekhi SF, Khademno A., Mechanical properties of cement mortar with Al₂O₃ nanoparticles. Journal of American Science, 2010; 6(4): 94-97.
- [13] Nazari A, Riahi Sh, Riahi Sh, Shamekhi SF, Khademno A., The effects of incorporation Fe₂O₃ nanoparticles on tensile and split tensile strength of concrete. Journal of American Science, 2010; 6(4): 90-93.
- [14] Nazari A, Riahi Sh, Riahi Sh, Shamekhi SF, Khademno A., Improvement the mechanical properties of the concrete by using TiO₂ nanoparticles. Journal of American Science, 2010; 6(4): 98-101.
- [15] Nazari A, Riahi Sh, Riahi Sh, Shamekhi SF, Khademno A., Embedded TiO₂ nanoparticles mechanical properties monitoring in cementitious composites. Journal of American Science, 2010; 6(4): 86-89.
- [16] Nazari A, Riahi Sh, Riahi Sh, Shamekhi SF, Khademno A., Benefits of Fe₂O₃ nanoparticles in concrete mixing matrix. Journal of American Science, 2010; 6(4): 102-106.
- [17] Nazari A, Riahi Sh, Riahi Sh, Shamekhi SF, Khademno A., Assessment of the effects of the cement paste composite in presence TiO₂ nanoparticles. Journal of American Science, 2010; 6(4): 43-46.
- [18] Nazari A, Riahi Sh, Riahi Sh, Shamekhi SF, Khademno A., An investigation on the Strength and workability of cement based concrete performance by using TiO₂ nanoparticles. Journal of American Science, 2010; 6(4): 29-33.
- [19] Nazari A, Riahi Sh, Riahi Sh, Shamekhi SF, Khademno A., Influence of Al₂O₃ nanoparticles on the split tensile strength and workability of blended concrete. Journal of American Science, 2010; 6(5): 6-9.
- [20] ASTM C150, Standard Specification for Portland Cement, annual book of ASTM standards, ASTM, Philadelphia, PA; 2001.
- [21] Zivica V. Effects of the very low water/cement ratio. Const Build Mater 2009; 23(8): 2846-2850.
- [22] Bui DD, Hu J, Stroeven P. Particle size effect on the strength of rice husk ash blended gap-graded Portland cement concrete. Cem Concr Compos 2005; 27(3): 357-366.
- [23] ASTM C496, Standard Test Method for Splitting Tensile Strength of Cylindrical Concrete Specimens, ASTM, Philadelphia, PA; 2001.
- [24] Tanaka K, Kurumisawa K.. Development of technique for observing pores in hardened cement paste. Cement and Concrete Research 2002; 32: 1435-41.
- [25] Abell AB, Willis KL, Lange DA. Mercury Intrusion Porosimetry and Image analysis of Cement-Based Materials. Journal of Colloid and Interface Science 1999; 211: 39-44.
- [26] Al-Khalaf MN, Yousift HA. Use of rice husk ash in concrete. Int J Cem Compos Lightweight Concr 1984; 6(4): 241-248.
- [27] Wu ZW, Lian HZ. High performance concrete. Beijing: Railway Press of China; 1999, p43. (in Chinese).
- [28] Ye Q. The study and development of the nano-composite cement structure materials. New building materials 2001; (1): 4-6. (in Chinese).